

The LANS- α Model for Computing Turbulence

Origins, Results, and Open Problems

*Darryl D. Holm, Chris Jeffery, Susan Kurien, Daniel Livescu,
Mark A. Taylor, and Beth A. Wingate*

Over the last 50 years, numerous computational turbulence models have been proposed for obtaining closure. Obtaining closure means capturing the physical phenomenon of turbulence at computably low resolution, by mimicking the effects of the small scales on the larger ones without calculating them explicitly. The Lagrangian-Averaged Navier-Stokes alpha (LANS- α) model is the first to use Lagrangian averaging to address the turbulence closure problem. LANS- α modifies the nonlinearity of the Navier-Stokes equation, instead of its dissipation, thereby providing an alternative way to reach closure without enhancing viscosity. The LANS- α model arose from an educated guess, based on combining Lagrangian-averaged nonlinearity with Navier-Stokes viscosity. Its derivation from these first principles implied mathematical theorems for its solutions, thereby guaranteeing that the most basic properties of the flow

(energy transport, circulation, variability, instability, dissipation anomaly, and intermittency) at scales above the effective cutoff scale of alpha are all

modeled accurately. Mathematical analysis also proved that the LANS- α solutions converge to Navier-Stokes solutions in the limit as the

correlation length parameter (alpha) tends to zero, thereby establishing the LANS- α model's accuracy. Moreover, the model's

solutions for nonzero alpha possess a global attractor

whose fractal dimension is finite, thus guaranteeing that

the solutions are rigorously computable using finite

resolution. The theorem-based approach of the

LANS- α model has raised the mathematical

standards for deriving other computational models

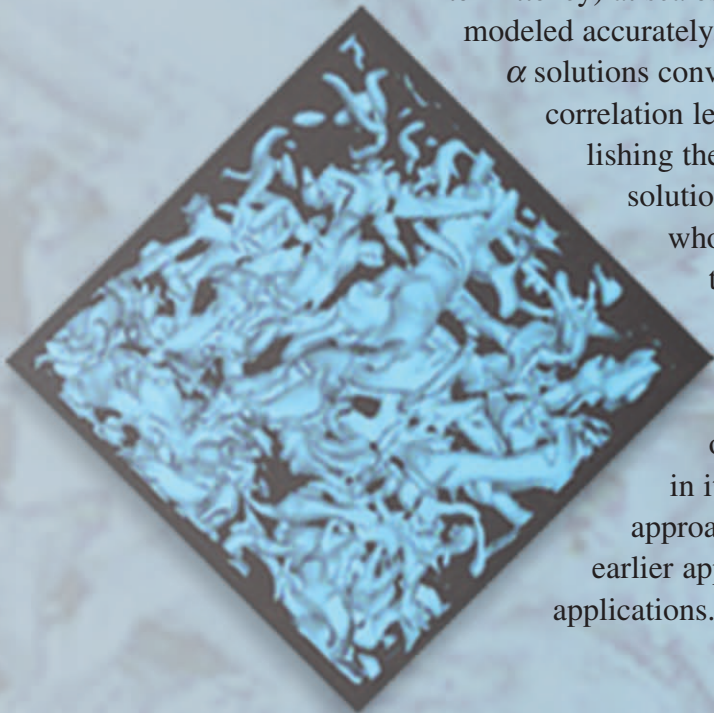
of turbulence. Application of the alpha model is still

in its infancy, but results so far suggest that this new

approach will complement, and in some cases subsume,

earlier approaches for modeling turbulence in real-world

applications.



Turbulence is an outstanding unsolved multiscale nonlinear problem of classical physics. It occurs spontaneously in a fluid, when forcing by stirring at the large scales gets transferred by nonlinearity into slender, swirling circulations in the flow. These coherent swirling “blobs” of fluid, pierced by vortex lines and bounded by material circulation loops are called eddies. The eddies are Lagrangian structures, that is, they travel with the flow, stretching themselves into extended shapes (sheets or tubes) as they follow the flow induced by the vortex lines that pierce them. The coherent eddies, sheets, and tubes of vorticity, stretching themselves into finer and finer shapes, comprise the “sinews” of turbulence.

The characteristic features of turbulence—its distribution of eddy sizes, shapes, speeds, vorticity, circulation, nonlinear convection, and viscous dissipation—may all be captured by using the exact Navier-Stokes equations. The Navier-Stokes equations correctly predict how the cascade of turbulent kinetic energy and vorticity accelerates and how the sinews of turbulence stretch themselves into finer and finer scales, until their motions reach scales of only a few molecular mean free paths, where they may finally be dissipated by viscosity into heat. However, the fidelity of the Navier-Stokes equations in capturing the cascade of turbulence is also their downfall for direct numerical simulations of turbulence.

The number of active degrees of freedom required to simulate the turbulent cascade in high-Reynolds-number flows quickly outstrips the numerical resolution capabilities of even the largest computer. To make turbulence computable, scientists have developed various approximate models that halt

Opposite page: The sinews of turbulence are illustrated by level surfaces of vorticity calculated with the LANS- α model at a spatial resolution of 256³.

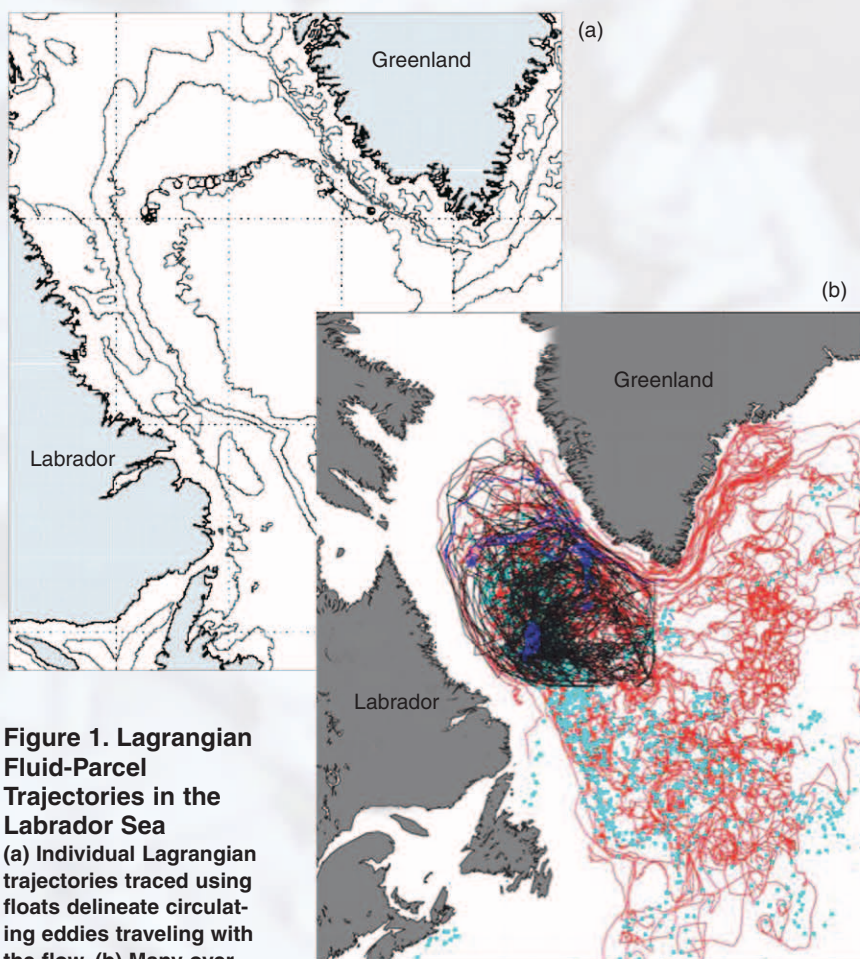


Figure 1. Lagrangian Fluid-Parcel Trajectories in the Labrador Sea

(a) Individual Lagrangian trajectories traced using floats delineate circulating eddies traveling with the flow. (b) Many overlapping trajectories capture the tangle of motions present in the flow.

(Permission granted by Gerd Krahnmann, Lamont-Doherty Earth Observatory of Columbia University.)

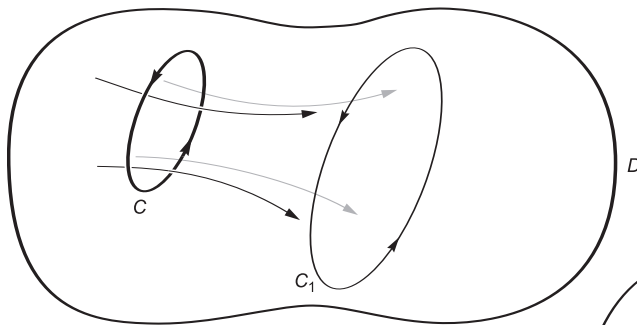
the cascade into smaller, faster eddies. In most models, this effect is accomplished by causing the eddies below a certain size to dissipate computationally into heat. This dissipative imperative causes errors, however, because it damps out the variability in the larger-scale flow caused by the myriad of small scales of motion interacting nonlinearly together in the fields of the larger motion.

Consider the problem of modeling the average effects of turbulence on ocean currents in the North Atlantic Ocean. The North Atlantic contains circulations ranging in size from thousands of kilometers to only a few meters. The variability in the flow has been documented through observa-

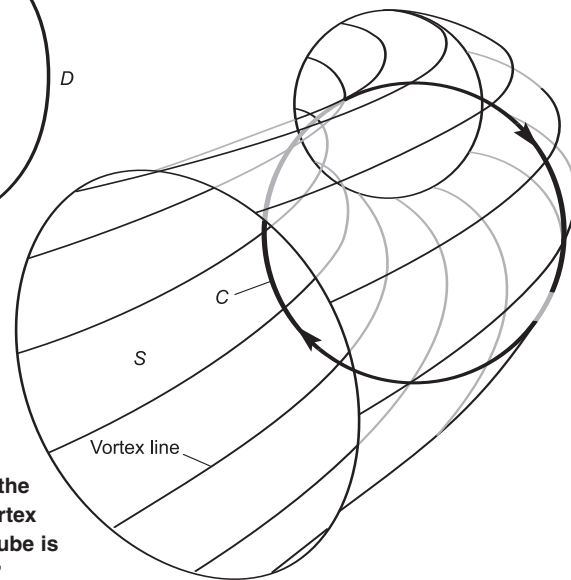
tions of Lagrangian trajectories (trajectories moving with the fluid parcels) in the Labrador Sea. As shown in Figure 1 (Krahnmann and Visbeck 2003), the Labrador Sea is full of highly oscillatory Lagrangian trajectories delineating the circulating eddy activity at the “mesoscale” size of tens of kilometers. Standard turbulence models for ocean simulations remove the fluctuating effects of all the scales of motion smaller than about 30 to 100 kilometers. Thus, the energy and information from the smaller scales are lost, and the resulting models ultimately are overdamped and inaccurate to the extent that the variability of their solutions depends upon these smaller scales.

The Lagrangian Eddy

A fluid possesses circulation if the integral of the tangential component of its velocity around any closed loop moving with the fluid is nonzero. A geometrical object such as a circulation loop embedded in, or traveling with, the fluid flow is an example of a Lagrangian quantity. A theorem of vector calculus by Kelvin and Stokes links the fluid's circulation with its vorticity, defined as the curl of its velocity. Namely, the circulation integral around the Lagrangian loop moving with the fluid is equal to the integral of the normal component of the fluid's vorticity, taken over any surface which has the circulation loop as its boundary. (This surface integral defines the "vorticity flux" through the surface whose boundary is the circulation loop.) Thus, circulation loops enclose distributions of vorticity flux, which may be regarded as bundles of vortex lines embedded in the fluid and wrapped by these Lagrangian circulation loops. These Lagrangian structures are known as "eddies." When the eddies stretch themselves into tubes, they are called "vortex tubes".



Above: As a material loop initially at C is carried by the fluid flow, it deforms to C_1 at a later time in domain D .



Right: A vortex tube is a material surface S surrounding a bundle of vortex lines (that is, lines tangent to the vorticity). The surface S is formed by a union of material loops C , each carried by the fluid flow. The divergence theorem implies that the flux of vorticity is the same through any slice, all along the vortex tube. Kelvin's theorem implies this flux of vorticity along the tube is constant in time. Thus, vortex tubes are "coherent structures."

(Redrawn from J. E. Marsden and T. S. Ratiu, *Geometric Analysis Methods in Fluid Mechanics*, manuscript in preparation.)

Capturing the mean effects of the smaller-scale circulations on the larger-scale motions in turbulence is called closure. In a novel approach, the Lagrangian-Averaged Navier-Stokes alpha (LANS- α) model we discuss here provides closure by modifying the nonlinearity in the Navier-Stokes equations to stop the cascading of turbulence at scales smaller than a certain length, but without introducing extra dissipation. Statistically, the size alpha in the LANS- α model is the typical distance that a Lagrangian trajectory fluctuates away from its time-mean tra-

jectory. Hence, by definition, alpha is the smallest eddy scale still participating actively in the cascade. Eddies at scales smaller than alpha are, in effect, slaved to the mean motions of the larger ones; that is, they fluctuate locally as they are carried along in the frame of motion of the larger scales. This modification of the Navier-Stokes nonlinearity, derived by applying Lagrangian averaging techniques, allows the turbulence problem to remain computable at the resolution size of alpha, but to still retain the mean circulation effects of the smaller

(subgrid) scales on the resolved solution. The LANS- α model is the first turbulence closure model to use Lagrangian averaging, from which it derives its name.

We shall briefly review the development of the LANS- α model from 1992 to 1997, catalog its key results from 1997 to 2004, and finally discuss the open problems. The year 1997 was a turning point because only then was it realized that the ideas being developed in the context of ocean modeling had the potential to be used as a computable turbulence model.

The Development of the LANS- α Model

The origins of the LANS- α model can be traced to a one-dimensional model of nonlinear shallow-water wave dynamics, written down in a moment of inspiration on a blank page, in a pocket calendar, during a seminar in 1992 at the Center for Nonlinear Studies. Researchers began to take the equation seriously when it was discovered to be a soliton equation. That is, its initial value problem was found to possess exact nonlinear (weak) solutions, playfully dubbed “peakons” because of their sharp peaks, whose motion and interactions could be completely solved using elastic collision rules (Camassa and Holm, 1993). Subsequently, the equation was derived from Hamilton’s principle of least action, which allowed it to be generalized to higher dimensions. The synergy between variational principles for soliton mathematics and dynamical concepts for turbulence modeling was developed further in the context of geophysical fluid dynamics, using a variety of approaches, including dominant asymptotics (Camassa et al. 1996, 1997).

The dominant asymptotics technique produces hierarchies of equations that, at each increasing order in the asymptotic expansion, include more physics. Between 1993 and 1996, an interesting relation was discovered between standard dominant asymptotics and asymptotics performed on the Lagrangian in Hamilton’s principle (HP). Namely, applying asymptotics in HP (before taking its variation) introduces terms in the resulting equations of motion that would ordinarily be dropped in dominant asymptotics, but which restore important fluid dynamical properties. These properties include conservation of both energy and potential vorticity (which arise from

symmetries of the Lagrangian in HP) in the absence of viscosity, and preservation of Kelvin’s theorem, which insures the proper nonlinear dynamics of circulation.

In 1996, Ivan Gjaja and Darryl Holm took the HP asymptotics idea a step further, while working on wave–mean flow interaction (WMFI) theory for ocean dynamics. WMFI theory addresses, for example, how surface waves can transfer momentum into regions far from their source. By applying Lagrangian averaging, as well as HP asymptotics, to a Wentzel-Kramer-Brillouin (WKB) wave packet representation of the rapid fluctuations, they derived the Gjaja-Holm WMFI equations, an asymptotic hierarchy of new equations for the wave–mean flow interaction. (Lagrangian averaging has a double meaning here because Gjaja and Holm averaged the Lagrangian in HP over the rapid phases of the WKB circulations at fixed Lagrangian coordinates.) Remarkably, these equations coincided with the result of applying dominant asymptotics and Lagrangian averaging to the exact Euler-Boussinesq equations for rotating, stratified, incompressible flows of an ideal fluid. This meant that the conservation laws for the Gjaja-Holm WMFI equations were programmed into the Lie-group symmetries of an averaged Lagrangian.

The Gjaja-Holm WMFI equations were developed in the context of the Laboratory’s Climate Change Prediction Program, led by Robert Malone. They were intended to provide a turbulence model for rotating stratified fluids such as the oceans and the atmosphere. However, these WMFI equations were quite different from the usual turbulence models, and they needed to be simplified considerably before they could be recognized as a turbulence model. The inviscid part of the simplification was proposed in 1997, in work by Darryl

Holm, Jerry Marsden, and Tudor Ratiu (1998a, 1998b). In this work, the Lagrangian-averaged Euler-alpha (LAE- α) equations, a Lagrangian-averaged closed form of the Euler equations (Navier-Stokes without viscous dissipation), were obtained. The key step in obtaining these LAE- α equations was the assumption of Taylor’s “frozen-in” hypothesis, namely, that the mean statistics of the rapid fluctuations were carried along, or frozen, into the Lagrangian mean flow instead of propagating as wave packets, as had been assumed in deriving the Gjaja-Holm WMFI equations. Nonetheless, the parameter α^2 in the LAE- α equations has the same meaning as it does in the Gjaja-Holm WMFI equations. That is, α^2 is the typical size (statistical correlation length) of the excursions of a fluid parcel trajectory away from its mean (phase-averaged) trajectory, where the phase average is taken at a fixed Lagrangian coordinate along that trajectory. The derivation of the LAE- α equations using this form of Taylor’s hypothesis is discussed in “Taylor’s Hypothesis, Hamilton’s Principle, and the LANS- α Model for Computing Turbulence” on page 172.

Once the LAE- α equations were derived, the stage was set for introducing viscosity and interpreting the resulting equations as a turbulence model. This last step in deriving the LANS- α model was taken in the collaboration among Shiyi Chen, Ciprian Foias, Darryl Holm, and Edriss Titi (1997–1998), when Foias, Titi, and their students Eric Olson and Shannon Wynne were visiting scholars at the Laboratory’s Center for Nonlinear Studies (CNLS) and Institute for Space and Planetary Physics (IGPP). The introduction of viscosity was made first on an ad hoc basis, and then the LANS- α model was interpreted and confirmed as a turbulence model by comparing its predictions with experiment and

numerical simulations and by analyzing its theoretical properties.

How the LANS- α Model Differs from Others

As mentioned above, the key difference between the LANS- α model and other models of turbulence arises from the difference in the averaging technique used to derive the nondissipative LAE- α equations. In the LANS- α model, the average effects of the small scales on the large are modeled in the Lagrangian frame, which moves with the fluid parcels, instead of being modeled in the Eulerian frame, which is fixed in space. The Lagrangian averaging procedure leads to a new closure mechanism, a mechanism which reduces the number of degrees of freedom in the turbulence problem and approximates the effects of the small scales on the large. That new closure mechanism is based on nonlinear transport. In contrast, the more traditional Eulerian-averaging procedure leads to closure through linear or nonlinear diffusion.

Traditional Eulerian turbulence models use the Reynolds decomposition to separate the fluid velocity \mathbf{u} at a point \mathbf{x} into its mean and fluctuating components as $\mathbf{u} = \bar{\mathbf{u}} + \mathbf{u}'$, where $\bar{\mathbf{u}}' = 0$ and the overbar denotes an Eulerian mean (time average at a fixed point in space). Mathematically, Eulerian averaging commutes with the partial derivatives in space and time, but it does not commute with the advective, or material, time derivative $D/Dt = \partial/\partial t + \mathbf{u} \cdot \nabla$. This lack of commutivity between Eulerian averaging and the material time derivative leads to the unknown Reynolds stresses in the motion equations for the Eulerian mean velocity $\bar{\mathbf{u}}$ and, subsequently, to the well-known closure problem (see page 132 of the article “The Turbulence Problem”). In contrast, Lagrangian averaging commutes (by

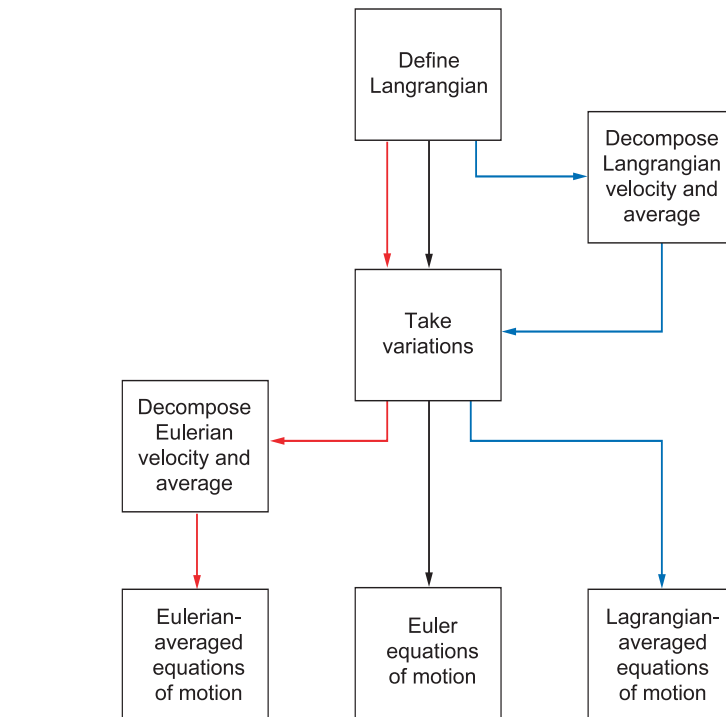


Figure 2. Paths to Derive Three Different Equations of Motion for Inviscid, Incompressible Fluid Flow

The blue path starts by decomposing the Lagrangian velocity into mean and fluctuating parts and then taking variations with respect to the Lagrangian averaged quantities to derive the LAE- α equations for ideal (inviscid) fluids.

definition) with the material time derivative to produce the generalized Lagrangian mean (GLM) equations. These GLM equations, however, are also not yet closed. Moreover, Lagrangian averaging does not commute with spatial gradients. As a result, the Lagrangian-mean theory is history dependent, preserving the memory of its initial labeling along its Lagrangian trajectories, and the statistics of the Lagrangian-trajectory fluctuations must be prescribed in order to close the GLM equations.

Figure 2 illustrates the paths taken to derive three different sets of equations: the Euler equations for inviscid, incompressible flow (black), the corresponding Eulerian-averaged equations for the mean motion (red), and the inviscid LAE- α equations (blue). To produce the exact Euler equations of motion, first the Lagrangian in Hamilton’s principle for fluids is

defined and then the variations of the action (that is, the time integral of the Lagrangian) are taken. In turbulence models based on Eulerian averaging, most of the modeling effort takes place after Hamilton’s principle of stationary variations of the action has produced the equations of motion. For Reynolds-averaged turbulence models, the velocity is then decomposed into its (Eulerian) mean and fluctuating quantities, or for the large eddy simulation (LES) framework, the equations in the Eulerian frame are spatially filtered. In contrast, for the LAE- α framework, the modeling occurs in averaging the Lagrangian in Hamilton’s principle before the variations are taken, and the Lagrangian-averaged equations result from taking variations of Lagrangian-averaged quantities using the Euler-Poincaré theory of Holm et al. (1998a, 1998b). (The averaged Lagrangian approach is

The LANS- α Model Equations

The LAE- α equations are

$$\frac{\partial \mathbf{v}}{\partial t} + \underbrace{\mathbf{u} \cdot \nabla \mathbf{v} + \nabla \mathbf{u}^T \cdot \mathbf{v}}_{\text{Modified nonlinearity}} + \nabla p = 0, \quad (1)$$

$$\text{with } \nabla \cdot \mathbf{u} = 0, \text{ and } \mathbf{v} = (1 - \alpha^2 \Delta) \mathbf{u}. \quad (2)$$

Rewriting Equation (1) as the time rate of change of momentum in the frame of the moving fluid yields

$$\frac{d}{dt} [\mathbf{v}(t, \mathbf{x}(t)) \cdot d\mathbf{x}(t)] + \nabla p \cdot d\mathbf{x}(t) = 0 \text{ along } \frac{d\mathbf{x}}{dt} = \mathbf{u}(t, \mathbf{x}(t)). \quad (3)$$

Adding viscosity and forcing yields the LANS- α equations:

$$\frac{\partial \mathbf{v}}{\partial t} + \underbrace{\mathbf{u} \cdot \nabla \mathbf{v} + \nabla \mathbf{u}^T \cdot \mathbf{v}}_{\text{Modified nonlinearity}} + \nabla p = \underbrace{\nu \Delta \mathbf{v} + \mathbf{f}}_{\text{Viscosity \& forcing}}, \quad (4)$$

$$\text{with } \nabla \cdot \mathbf{u} = 0, \text{ and } \mathbf{v} = (1 - \alpha^2 \Delta) \mathbf{u}. \quad (5)$$

The Kelvin circulation theorem for the LANS- α model is

$$\frac{d}{dt} \oint_{c(\mathbf{u})} \mathbf{v} \cdot d\mathbf{x} = \oint_{c(\mathbf{u})} (\nu \Delta \mathbf{v} + \mathbf{f}) \cdot d\mathbf{x}. \quad (6)$$

much simpler and more transparent than averaging the equations term by term, and a theorem guarantees that the same equations result in either order. A concise description of this process is given in the article “Taylor’s Hypothesis, Hamilton’s Principle, and the LANS- α Model for Computing Turbulence” on page 172.) The LAE- α equations (in terms of Eulerian averaged quantities) are given by Equations (1) and (2) in the box above.

The two velocities \mathbf{u} and \mathbf{v} in the LAE- α Equations (1) and (2) are averaged quantities. However, the transport velocity \mathbf{u} is smoother than the transported velocity \mathbf{v} by inversion of the Helmholtz operator, $(1 - \alpha^2 \Delta)$.

This inversion operation amounts to obtaining velocity \mathbf{u} by filtering velocity \mathbf{v} over the length scale α . When $\alpha \rightarrow 0$, then $\mathbf{v} \rightarrow \mathbf{u}$, and one recovers the original Euler equations.

According to the Euler-Poincaré theory of Holm et al. (1998a, 1998b), the transport velocity \mathbf{u} in Equation (1) is the average velocity at which the fluid material moves. So, what is the interpretation of the other average velocity \mathbf{v} in Equation (2)? The Euler-Poincaré theory defines the velocity \mathbf{v} as the momentum per unit mass of the Lagrangian averaged motion. This momentum is obtained by taking the variational derivative of the averaged Lagrangian in Hamilton’s principle with respect to the average velocity \mathbf{u} .

The two velocities differ for the usual reason, namely, that nonlinearity and averaging do not commute. One may understand the different roles of these two velocities by considering the LAE- α equation as a form of Newton’s law for the time rate of change of the momentum in the frame of fluid motion. Namely, Equation (1) is equivalent to Equation (3). Thus, the second term in the modified nonlinearity of Equation (1) arises from the rate of change of the line element $d\mathbf{x}(t)$ in the frame of motion of the fluid moving with velocity \mathbf{u} . (Of course, the first term in this nonlinearity arises from the chain rule.)

After deriving these inviscid LAE- α equations, we added viscosity and forcing so that energy would decay and momentum would diffuse, thereby obtaining the LANS- α model Equations (4) and (5). When $\alpha \rightarrow 0$, then $\mathbf{v} \rightarrow \mathbf{u}$ and the LANS- α equations revert to the original Navier-Stokes equations.

Remarkably, the LANS- α equations answered an outstanding mathematical question going back to the early efforts of Leray (1934) to regularize the Navier-Stokes equations. This question was emphasized by Galovotti (1993), namely, “How does one regularize the Navier-Stokes equations without destroying their circulation properties?” (Recall that the LANS- α model was developed to deal with average effects of turbulence in ocean circulation.) The answer is obtained by direct calculation, which yields the Kelvin circulation theorem for the LANS- α equations given by Equation (6). Physically, this theorem means the circulation of the velocity \mathbf{v} around a material loop c moving with smoothed transport velocity \mathbf{u} is created by the integral around this loop c of the sum of the viscous and external forces. When $\alpha \rightarrow 0$, then $\mathbf{v} \rightarrow \mathbf{u}$, and one recovers the fundamental Kelvin circulation theorem for the Navier-Stokes equations, thereby regaining

the picture of the sinews of turbulence described earlier. The Kelvin circulation theorem for the LANS- α equations above shows how this picture is modified by Lagrangian averaging. We will discuss later how the LANS- α Equations (4) and (5) regularize the Navier-Stokes equations in the sense discussed by Leray (1934) and Galovotti (1993).

Results from 1997 to 2004

In the next few sections, we present a sampling of key results for the LANS- α model from 1997 to 2004. This is not meant to be an exhaustive review of the entire body of the LANS- α literature, but a sampling of theoretical and numerical results to give the reader a flavor for what is known and what remains to be studied.

Through the rest of this article, the word ‘modeling’ refers to the mathematical description of unknown quantities in terms of known quantities for the purpose of regularizing or reducing the number of active degrees of freedom in the Navier-Stokes equations.

“Benchmark” Tests of the LANS- α Model

Once we recognized that LANS- α might be interpreted as a turbulence model, we tested this hypothesis by using LANS- α to calculate some of the classic turbulence problems. These included turbulent flow in a pipe, forced turbulence in a periodic domain, and decay of turbulence in a periodic domain. In all three cases, the results were very encouraging.

LANS- α Stationary Solutions for Pipe Flow Compared with Experimental Data. Figure 3 (Chen et al. 1999a) shows a semilog plot of

the time-averaged velocity for turbulent flow in a pipe vs distance from the wall at three different Reynolds numbers. The experimental data (solid lines) were measured at the Princeton “super pipe” and correspond to turbulent flows with the highest values of Reynolds number available in a pipe-flow experiment (Zagarola 1996). The dashed lines show the corresponding stationary solutions of the LANS- α model. All three solutions were obtained using a single constant value of alpha (equal to about one percent of the pipe radius). This value of alpha was obtained by matching the first set of data at a Reynolds number of 98,812. Then, alpha was held constant for the other two comparisons. The family of mean velocity profiles $\phi(\eta)$ seems to possess a lower envelope. This straight line in the semilog plot satisfies the famous von Kármán logarithmic law of the wall. However, the LANS- α steady solutions match the experimental data all the way across the pipe flow domain, from a few tens of wall units away from the pipe boundary all the way to the pipe center, where the peak of each curve occurs. (These peaks are offset because the wall unit η contains the Reynolds number in its definition.)

Note that the LANS- α solution matches the measured mean velocity over many orders of magnitude in wall units. That agreement is a good sign because turbulence models must describe a wide range of scales of motion—from the scale of the forcing down to the dissipation scale. The faint, dotted lines show the recent power law from Barenblatt-Chorin (1997), which does not capture the peaks of the curves. The excellent agreement with the experimental mean velocity profiles (from Chen et al. 1998, 1999a) provided the first clue that the LANS- α equations for the Lagrangian mean velocity might be interpretable as a model of turbulence.

Navier-Stokes Equations: Forced Turbulence in a Periodic Domain.

Next, we tested the LANS- α model on the problem of forced turbulence in a three-dimensional (3-D) periodic domain where turbulence is approximately homogeneous and isotropic so that Kolmogorov-like scaling laws should obtain. We performed direct numerical simulations of the LANS- α model and examined the effect of increasing alpha on the energy spectrum $E(k)$, where k is the wave number. Results from Chen et al. (1999) show that, in the spectral region $k\alpha < 1$ (that is, for spatial scales larger than alpha), $E(k)$ is proportional to $k^{-5/3}$, as expected for homogeneous, isotropic turbulence. In other words, the energy spectrum at these spatial scales is essentially unaffected by the presence of the α -modification (regularization). However, in the spectral region with $k\alpha > 1$ (that is, for spatial scales smaller than alpha), $E(k)$ rolls off faster as wave number increases. In Chen et al. (1999b), we kept alpha fixed at $\alpha = 1/8$ of the domain size and compared the energy spectrum for a high-resolution mesh of 256^3 cells and a low-resolution mesh of 64^3 cells. The energy spectra at the large scales (in the inertial range) were the same for both simulations, which means that, for this problem of forced turbulence, the large-scale flow properties can be preserved when the resolution is decreased by a factor of 8. (The actual computational savings is a factor of about $4^4 = 256$ in computer time.) This result implies that direct numerical simulation of the LANS- α model allows a significant computational savings over the direct numerical simulation of the Navier-Stokes equations.

Later, Foias et al. (2001) used dimensional arguments to predict the faster energy-spectrum rolloff for $k\alpha > 1$ that was seen in the computations. These dimensional arguments predict-

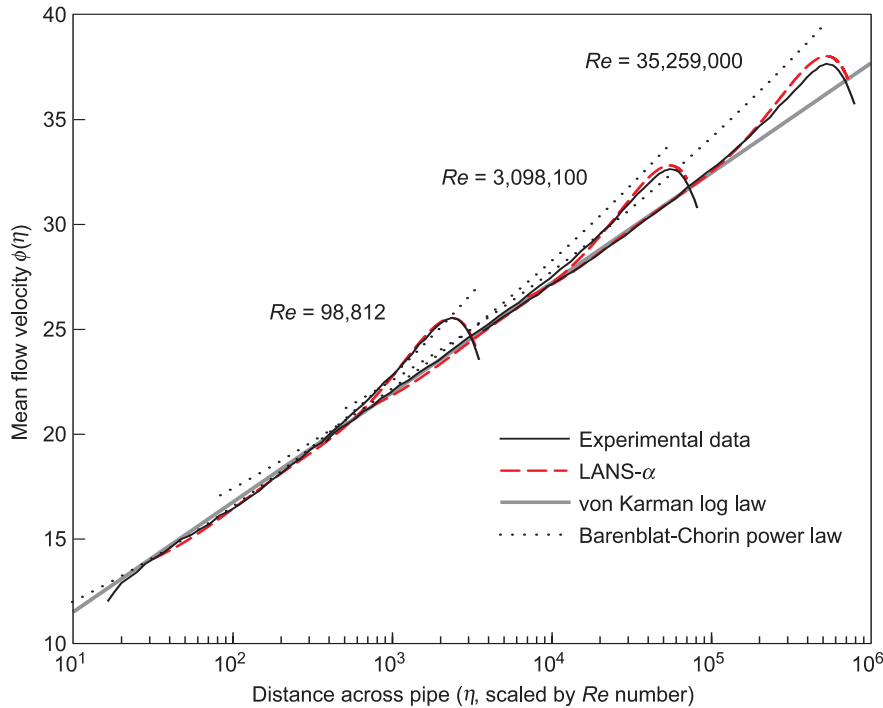


Figure 3. Mean Velocity Profiles for Pipe Flow
 Comparison in this figure from Chen et al. (1998, 1999a) of mean flow profiles for turbulent flow in pipes given by experimental data shows reasonable agreement with the profile of the corresponding solution of the LANS- α equations at the highest experimentally available Reynolds numbers. Here, the mean-velocity profile in the pipe for the LANS- α equation (the red dashed line) is compared with the experimental data (the solid line) of Zagarola (1996). (Copyright 1998 by the American Physical Society.)

ed the rolloff to be $k^{-5/3} \rightarrow k^{-3}$ for the LANS- α model. The rolloff $k^{-5/3} \rightarrow k^{-3}$ is consistent with the Re^2 scaling behavior in computational work for a fully resolved direct numerical simulation of the LANS- α equations, in comparison with the Re^3 scaling behavior in computational work for a fully resolved direct numerical simulation of the Navier-Stokes equations.

The relative scaling of Re^2 for LANS- α vs Re^3 for the Navier-Stokes equations implies a two-thirds-power scaling in the computational work required in the direct numerical simulation of the Lagrangian-averaged LANS- α equations vs the exact Navier-Stokes equations, provided the k^{-3} inertial range for the LANS- α model is resolved. At a large Reynolds number, Re , this scaling can provide a substantial savings in computational work.

Navier-Stokes Equations: Turbulence Decay in Three-Dimensions. A more stringent test of the LANS- α model is the initial value problem for 3-D incompressible turbulence known as turbulence decay. In this problem, one starts from a turbulent initial condition that results from forcing, and then one turns off the forcing and lets the turbulence decay away. In recent computations (Holm and Kerr 2002; Geurts and Holm 2002a, 2002b; Mohseni et al. 2000, 2001), numerical comparisons between large-eddy simulation (LES) methods and the LANS- α model were made for the onset, development, and decay of shear turbulence. All three of these numerical studies compared the predictions of the LANS- α model for the case of shear turbulence decay in three dimensions against the most

advanced LES models, which achieve closure through modifying the energy diffusion rather than the nonlinearity. The standard of comparison for these low-resolution model simulations using the LANS- α model and several standard LES approximate models was a direct numerical simulation of the full Navier-Stokes equations at a much higher resolution. In these investigations, Holm and Kerr started from a Taylor-Green initial condition specified by spectral data; Geurts and Holm started from the classic physical realization of the Kelvin-Helmholtz instability, leading to the formation and decay of turbulent shear layers; and Mohseni et al. studied the decay of turbulence in the standard Comte-Bellot and Corrsin wind-tunnel configuration.

In all these benchmark problems, the results of the Lagrangian-averaging approach to modeling turbulence were found to be comparable with the best of the standard LES approximate models.

Relation of LANS- α Model to Large-Eddy Simulations

LES models are often used in numerical simulations of turbulence. Because of their importance and their formal similarity to LANS- α , considerable work has been devoted to understanding the connection between LANS- α and LES.

The basis for the LES approach is spatial filtering of the Navier-Stokes equations in the Eulerian frame, whereas the theoretical basis for obtaining the LANS- α equations is Lagrangian averaging. Of course, both approaches face difficulties with closure. Either approach to closure introduces approximations because the equations are nonlinear, and neither the averaged nor the filtered product of two factors would be equal, in general, to the product of the averaged, or filtered, factors.

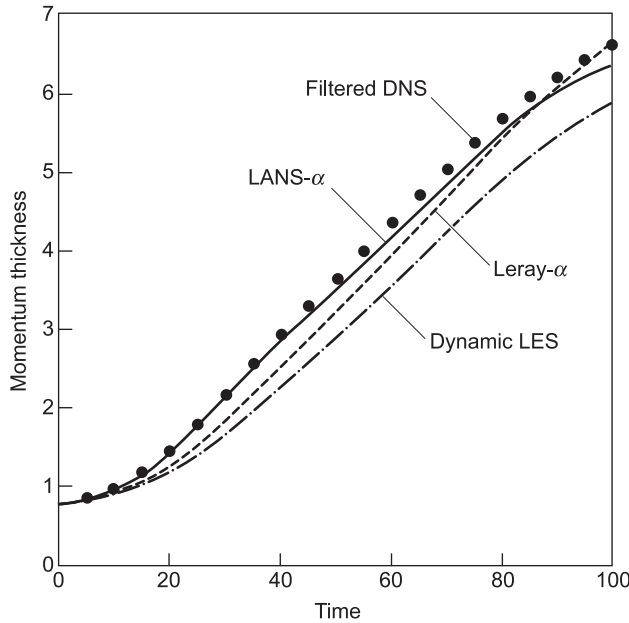


Figure 4. Comparing Results of LANS- α and Leray- α with Dynamic LES for the Turbulent Mixing Layer

This figure from Geurts and Holm 2002 compares the momentum thickness as a function of time for the turbulent mixing layer initiated by the Kelvin-Helmholtz instability. Here $\alpha = L/16$ and three LES models are plotted: LANS- α (solid), Leray- α (dashed), Dynamic LES (dash-dotted). The nearly grid independent DNS solution at resolution is shown as solid circles. The momentum thickness for the mixing layer begins with a strong convective surge, which the LANS- α model follows well. The Leray- α model lacks the term that provides line-element stretching to complete Kelvin’s circulation theorem, and apparently this term is important at an early time. Dynamic LES apparently lags in the beginning and never catches up, perhaps because it attempts to model nonlinear turbulent transport as diffusion.

(Reprinted with the permission of Springer-Verlag.)

Formally, the Lagrangian-averaged turbulence equations appear similar to the LES turbulence equations (Domaradzki and Holm 2001), but there are significant differences in the interpretations of their solutions. These differences in interpretation arise because the two models are derived from different fundamental principles. The similarity between them arises because both approaches yield expressions for conservation, or balance, of momentum. The similarity between them also arises through interpreting the equations produced by the Lagrangian-averaging approach as embodying a “regularization principle,” which involves an explicit filter and its inversion (Guerts and Holm 2003). Momentum conservation for

this regularization principle identifies the stress tensor corresponding to the implied subgrid model, which resolves the closure problem. Thus, the model equations resulting from the Lagrangian-averaged turbulence method convey a central and very specific physical role to a filter: The transport velocity is a filtered version of the fluid momentum, including the mean momentum of the fluctuations. This role differs from that of the filter in the foundations of the LES approach. In the LES approach, the difference between the filtered product of velocities and the product of filtered velocities is modeled as a symmetric tensor involving gradients of the filtered velocity, whose divergence introduces dissipation of energy.

In terms of physical effects, the dissipation introduced by LES filtering smoothes and slows the fluid’s momentum, so the LES results tend to be sluggish compared to DNS and, thus, LES often fails to capture the true variability of turbulence. In contrast, the modification of the nonlinearity in the alpha model “enslaves” the smaller scales to the larger ones, and their circulation is not lost to heat. This feature gives the LANS- α model an advantage. For example, it produces sharper, more-pronounced coherent structures and higher variability than even the best LES models (the dynamic LES models) in computing turbulent shear mixing (see Figure 4).

Application of LANS- α to Specialized Problems

Thin-Layer Navier-Stokes

Equations: Self-Similarity. Steady self-similar solutions (for the dependence of mean downstream velocity U in a two-dimensional (2-D) boundary layer of the form $U(x, y) = g(x)f(y/x)$) of the thin-layer Navier-Stokes (TLNS) equations were known for laminar boundary-layer problems since Paul Blasius in 1908. For turbulent shear flows such as jets, wakes, and plumes, the Kelvin-Helmholtz instability generates mixing near the interface between the moving and stationary fluids, and the mixing region spreads transversely, as the unstable entrainment interaction between the fluids proceeds in time—see Figure 5(a). Finding solutions to these self-similar flows was plagued by closure problems until Ludwig Prandtl (1925) invented the mixing-length theory, which captures the drag effects of turbulent eddies. Prandtl’s mixing length is a macroscopic length scale defining the mean distance between eddy collisions; it was meant to be analogous to the mean free path

between molecules in kinetic theory. For most TLNS self-similar problems, such as jets, wakes, and plumes, analytical results from Prandtl's mixing length theory match experimental data reasonably well.

Except for that simple mixing-length theory, self-similar solutions of most turbulence models have not been investigated. However, because the LANS- α equations were derived to have self-consistent dynamics, such solutions seemed possible. Indeed, thin-layer self-similar solutions of the LANS- α model were found for boundary layers, jets, wakes, and plumes (Cheskidov 2002, Holm et al. 2003, Putkaradze and Weidman 2003). These solutions arise by introducing both α (a statistical property of Lagrangian averaging) and a mixing length (a statistical property of Eulerian averaging). Each averaging mechanism seems to control a different aspect of the analytical self-similar solutions. For example, in the planar jet shown in Figure 5(a), the thickness of the jet $g(x)$ depends only on x , the distance downstream from the source, and that thickness is determined entirely by mixing-length theory. On the other hand, the profile of the analytical solution for the mean velocity U across the jet—see Figure 5(b)—is a function of the similarity variable, $\eta = y/x$, and the shape of that profile is determined by α in these calculations. Figure 5(b) also shows a comparison of the alpha model's similarity solution with the experiments of Effie Gutmark and Israel Wygnanski (1976).

Understanding the interplay of diffusion (as in the mixing-length theory) and transport (as in the LANS- α model) is still an outstanding problem in modeling these self-similar turbulent flows.

Geophysical Fluids. Geophysical fluid dynamics offers a unique regime in which to compare the LANS- α

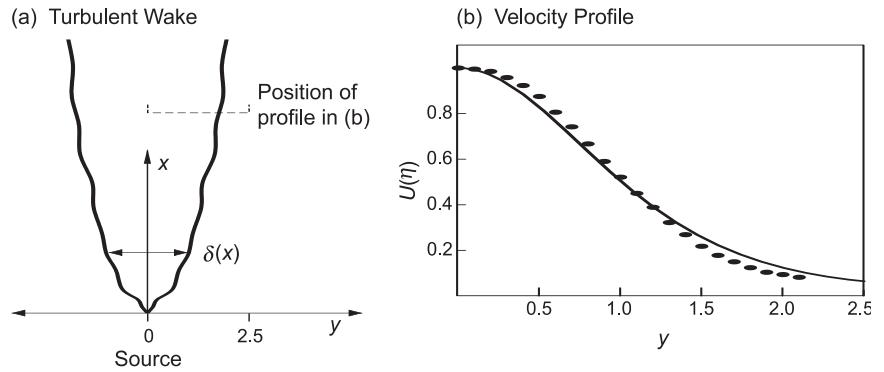


Figure 5. Self-Similar Solutions for a Planar Turbulent Jet
(a) A turbulent jet gushes out from a source. (b) The analytical solution of the LANS- α equations for a planar turbulent jet is compared with results from experiments) by Gutmark and Wygnanski (1976).

(Reprinted with the permission of Cambridge University Press.)

model with other well-known models because the energy does not cascade to the small scales as it does in 3-D incompressible Navier-Stokes turbulence. Instead, these quasi-2-D flows are characterized by an upscale transfer of energy to lower wave numbers. This transfer of energy creates the large-scale vortices observed in nature. As a consequence, coarse-resolution models have a good chance of simulating the most important dynamical features of these flows. Between 1997 and 2004, two important regimes were studied: quasi-geostrophy, whose principal wave solutions are slow-time-scale Rossby waves, and the rotating shallow-water equations, whose solutions include both Rossby waves and fast inertial waves.

Quasi-Geostrophy (QG).

Application of the LANS- α model to slow, large-scale motions for rotating, planetary-scale fluid dynamics has yielded mixed results. Two sets of simulations have been performed of the problem of wind-forced circulation in a closed ocean basin. Wind-forced circulation results, ostensibly, in two counter-circulating gyres. As described in Greatbatch and Nadiga (2000), the time-mean ocean basin circulation predicted by the QG equa-

tions shows a four-gyre pattern, although its instantaneous motion generally shows only two gyres, which fluctuate strongly and rapidly.

In the low-resolution LANS- α simulations of Nadiga and Margolin (2001), the four-gyre time-mean pattern was recovered, but only after an appropriate combination of alpha and dissipation parameters were determined from a higher-resolution eddy-resolving run (regarded as a direct numerical simulation). Further, the correspondence between the time mean of the eddy-resolving run and the α -parameterized run was less than satisfactory and not fully understood. This incompleteness left open questions that still need further study.

In Holm and Nadiga (2003), an LES viewpoint was adopted, in which low-resolution simulations of the QG- α model and some of its close variants were compared with time means of direct numerical simulations of QG for the full double-gyre problem. This approach led to significantly improved results for the time-mean circulation in the double-gyre problem, and it also captured reasonable variability in the form of eddy kinetic energy and eddy potential enstrophy. Figure 6 shows contour plots of the time-averaged stream function, in

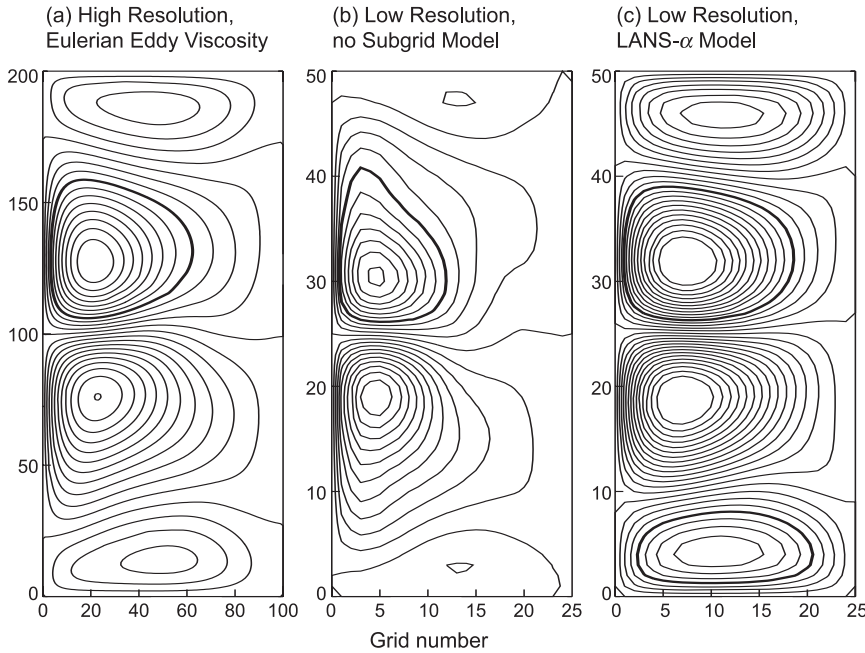


Figure 6. Quasi-Geostrophic Double-Gyre Problem

This figure from Holm and Nadiga (2003) shows time-averaged contour plots of the stream function for the quasi-geostrophic double-gyre problem. (a) Shown here is a 96^3 high-resolution QG simulation. The Munk layer scale is $0.02L$, and the grid resolution is $0.01L$. At this low level of viscosity, the time-mean stream function displays a four-gyre structure even though the wind forcing is that for a double gyre. (b) This simulation is run at a resolution that is 4 times coarser—a grid resolution of $0.04L$. With no modeling of the subgrid scales, we find that the outer pair of gyres is greatly weakened compared with the pair in (a). (c) This simulation is also run at a resolution that is 4 times coarser, but it uses the alpha model to account for subgrid scale activity. Here, we find that the outer pair of gyres is restored. However, the strength of the wind-driven and the eddy-driven mean circulation is slightly higher than the resolved simulation shown in (a). We are currently studying the reasons for this overprediction. (Permission granted by the American Meteorological Society.)

which the four-gyre pattern clearly emerges.

The results in Figure 6 show that the LANS- α model yields a decided benefit in predicting the correct time-mean variability for this problem. However, the strength of the circulation was slightly higher than in the resolved simulation.

Rotating Shallow Water (RSW).

Because RSW produces fast waves, the RSW equations are hard to solve numerically. The maximum allowable time step is $\Delta t \leq C/N$, where C is a constant of order unity and N is the number of mesh points in the domain.

Using the LANS- α model to simulate these equations led to a slowing down of the fastest waves (those with wave lengths smaller than α). Consequently, LANS- α simulations that used a much larger time step, given by $\Delta t^{(\alpha)} \leq C\alpha$, retained the high variability found in the highest-resolution runs. This means that refining the mesh with a fixed α causes the LANS- α model’s maximum allowable time step to go to a constant, while the shallow-water model requires its time step to go to zero.

These simulations also revealed that the LANS- α model preserves the time variability of the dynamics.

Figure 7 from Wingate (2004) shows the time series spectra for the kinetic and potential energy on two different grids for the double-gyre problem (see the caption for details).

Although the LANS- α model does reproduce the time variability of shallow-water flow, these results raise several questions. As shown in Figure 7, increasing α may cause an overprediction of variability, as discovered in the study of the double gyre in Nadiga and Holm (2003). This overprediction of variability leads us to ask, “How does one make an optimal choice of α ?” Also, for the same viscosity, the alpha model typically has a higher variability than coarse-resolution simulations of the exact equations. This increased variability occurs because, in the LANS- α model, the enstrophy-like energy (not the translational kinetic energy) controls dissipation at high wave numbers. This result brings up the question, “Should the Reynolds number be defined differently in these cases?” This issue will be addressed in the section on open problems.

Modeling Fluid Instability

The stability and instability of flows in different parameter regimes (such as Reynolds number Re , Rossby number Ro , and Froude number Fr) could be altered, in principle, by introducing turbulence models. We performed two studies of fluid instability in the LANS- α model.

Elliptical Instability. The elliptical instability converts 2-D fluid motions into 3-D convection, so it provides a fundamental mechanism at the onset of turbulence. Motivated by the idea that a turbulence simulation method should not erroneously predict stability in a flow that is actually unstable, Fabijonas and Holm (2003) investigated the elliptical instability in the

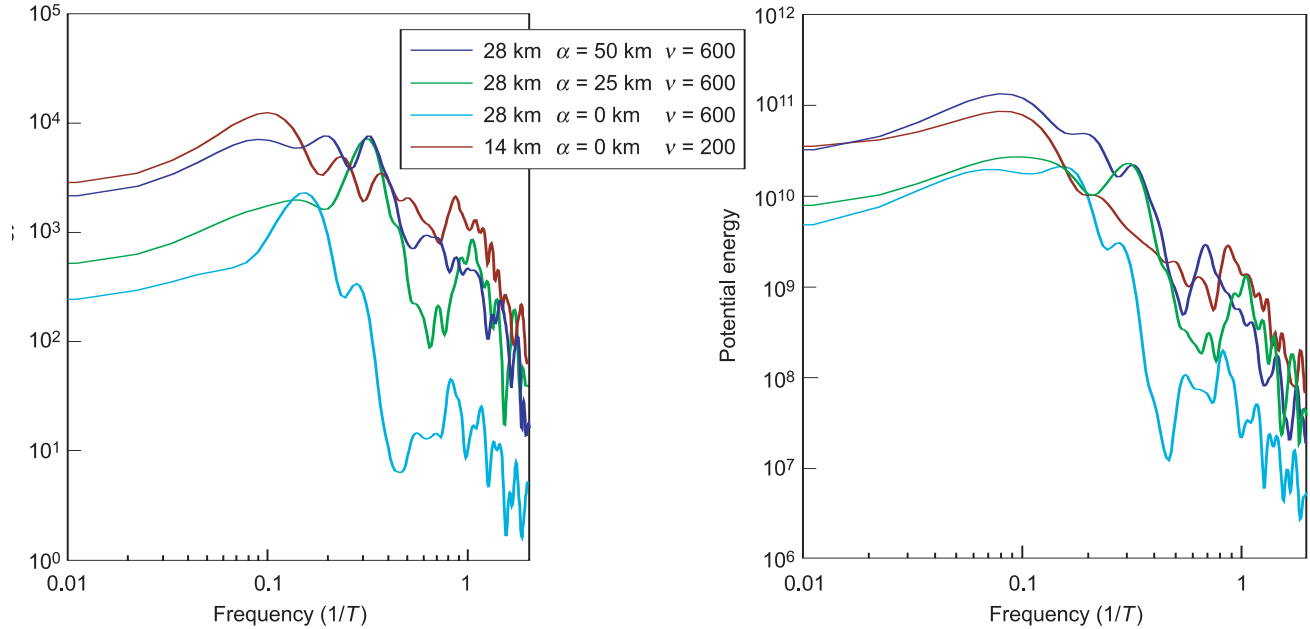


Figure 7. Improved Variability for LANS- α Shallow Water Simulations

(a) The kinetic energy is shown as a function of frequency; (b) the potential energy is shown as a function of frequency. In both (a) and (b), the values are for shallow water simulations at different values of α and different resolutions. The Rossby deformation radius for all cases is approximately 48 km. The high-resolution calculations (red) with $\alpha = 0$, an average grid spacing of 14 km that resolves the Rossby radius, and a viscosity of 200 m²/s serve as our standard of energy variability. The other three simulations were performed on a much coarser mesh with an average grid spacing of 28 km, a mesh size for which the Rossby deformation radius is not well resolved. The pale blue curve shows the results of the simplest eddy viscosity model ($\alpha = 0$ and just enough viscosity is added to prevent numerical instability). The flow is sluggish with almost an order of magnitude decrease in the variability of the kinetic energy due to the increase in the dissipation of the total energy. The purple curve shows the increased variability that results by introducing alpha at the value $\alpha = 25$ km. The dark blue curve shows that, by increasing alpha to the size of the Rossby deformation radius, we recover the variability of the fine-grid case.

LANS- α model and showed that the model preserves, but modifies, this important instability. In particular, the LANS- α model reduces the maximum growth rate for higher wave numbers, $k\alpha \gg 1$, but for slightly lower wave numbers, $k\alpha > 1$, the model increases the maximum growth rate. This enhancement allows the dynamics of the small scales to affect the larger scales. This work led to a sequence of investigations: from early assessments of the average effects of turbulence on elliptic instability to later assessments of the combined effects and interplay of turbulence, rotation, and stratification on elliptical instability.

Baroclinic Instability.

Investigations using global ocean models or coupled ocean, atmosphere,

and ice models require the use of coarse meshes. The meshes are often so coarse that the Rossby deformation radius is not resolved,¹ and consequently baroclinic instability is incorrectly predicted. Baroclinic instability is initiated by vertical shear in a rotating, stratified flow and describes the process of converting available potential energy to kinetic energy on scales of the Rossby deformation radius. This is one of the most important dynamical phenomena in geofluid dynamics and one that any turbulence model must reproduce if it is to simulate the correct variability.

¹ The Rossby deformation radius is the distance at which the pressure force balances with the Coriolis force in the motion equation.

In Holm and Wingate (2004), neutral curves for the onset of baroclinic instability from the simplest LANS- α model were compared with those from the simplest eddy-viscosity model (see Figure 8). Neutral curves show the shear forcing required to initiate baroclinic instability versus wave number. Figure 8(a) presents LANS- α neutral curves for three values of αk_{int} , the length of α relative to the Rossby deformation radius. As α , or αk_{int} , is increased, the critical wave number (wave number at the minimum of the neutral curve) shifts to lower wave number while the value of the minimum forcing required remains the same. Thus, the onset of baroclinic instability remains resolvable with fewer grid points. Figure 8(b) shows neutral curves for

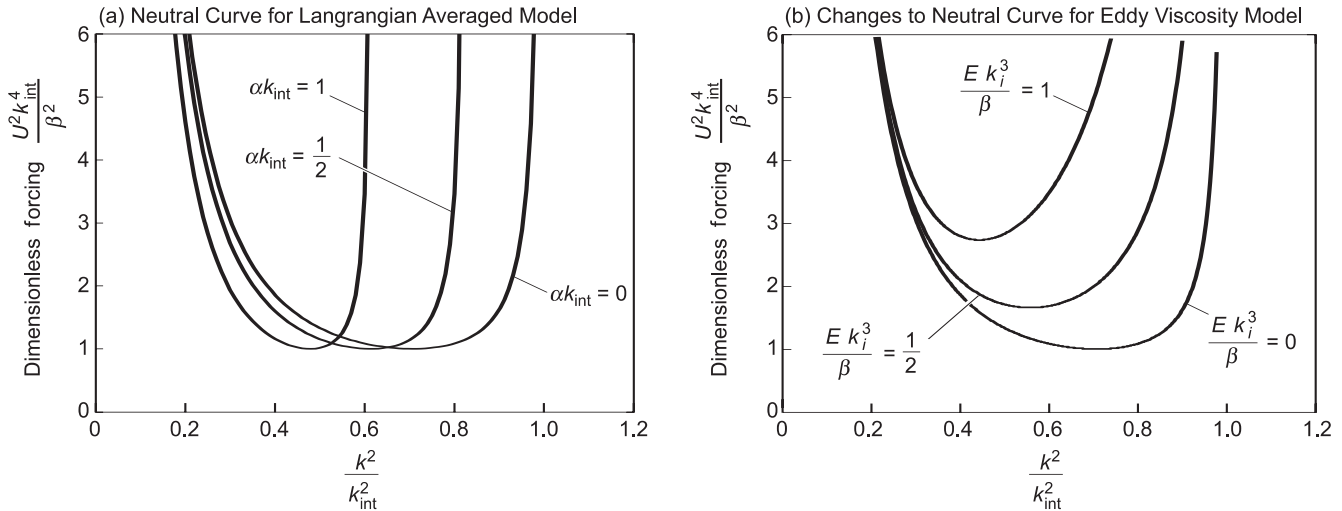


Figure 8. Baroclinic Instability: LANS- α vs Eulerian-Averaged Eddy Viscosity Models
 Neutral curves show the onset of baroclinic instability (Holm and Wingate 2004). U^2 is a measure of the strength of the shear, k_{int} is the wave number of the internal Rossby deformation wave, $\beta = df/dy$, where f is the coriolis parameter, and E is the eddy viscosity. Both models lower the critical wave number for the onset of instability (the value of k at the minimum point of these neutral curves) as the modeling parameter is increased. For LANS- α , the onset occurs at the same value of the forcing irrespective of the value of α . (b) For the eddy viscosity model, the onset requires higher forcing as E is increased because of the increase in dissipation.

the eddy viscosity model for three values of Ek_{int}^3/β . As the viscosity E increases, the critical wave number again decreases, but the minimum forcing for instability gets higher rather than remaining constant. This difference arises because the LANS- α model uses dispersion to lower the critical wave number, whereas the eddy-viscosity model uses energy dissipation. The eddy-viscosity model thus requires higher forcing for the onset of baroclinic instability, and consequently some of the instability that should be present in the flow is lost as E is increased. In the LANS- α model, the gradient of potential vorticity, which drives the instability, is preserved, and therefore baroclinic instability occurs at the same forcing values as those predicted by the exact Navier-Stokes equations.

What remains unanswered is how best to choose the parameter α and how to combine both eddy-viscosity models and Lagrangian averaging in concert to achieve the most realistic results in both global ocean models and in coupled ocean, atmosphere, and ice models.

Theoretical Developments for the LANS- α Model

The Kármán-Howarth Theorem for Dynamics of the LANS- α Model. The Kármán-Howarth theorem for fluid turbulence (1938) given by Equation 7 (see box) is an exact analytical relation between the time rate of change of the second-order two-point velocity correlation function and the gradient of the third-order two-point velocity correlation function derived from the Navier-Stokes equation for homogeneous, isotropic turbulence.

Equation (7) is the lowest-order two-point statistical equation for turbulence dynamics and may be understood as a relationship between the rate of change of energy in scales of size r to the flux of energy through scales of size r .

One can write the same equation for velocity structure functions, which are the moments of the longitudinal velocity difference, $\delta_L u(\mathbf{x}, t; \mathbf{r}) = \hat{\mathbf{r}} \cdot \delta \mathbf{u}(\mathbf{x}, t; \mathbf{r})$, with $\delta \mathbf{u}(\mathbf{x}, t; \mathbf{r}) \equiv \mathbf{u}(\mathbf{x} + \mathbf{r}, t) - \mathbf{u}(\mathbf{x}, t)$. One example is the second-order structure function $\langle [\delta_L u]^2 \rangle$. See the articles “The Turbulence Problem” and “Direct Numerical Simulations of

The Kármán-Howarth Theorem

$$\frac{\partial}{\partial t} \langle u_i(x) u_i(x+r) \rangle - \frac{\partial}{\partial r_j} \langle u_i(x) u_j(x) u_i(x+r) \rangle = 2\nu \frac{\partial^2}{\partial r_j \partial r_j} \langle u_i(x) u_i(x+r) \rangle \quad (7)$$

where subscripts i, j denote components in a Cartesian coordinate system. The gradient of the third-order two-point velocity correlation function (the second term) arises from the nonlinear term in the Navier-Stokes equations.

Turbulence” on pages 124 and 142, respectively, for further discussion of structure functions. Kolmogorov (1941a, 1941b) used the structure function form of the Kármán-Howarth equation to show that, for homogeneous, isotropic, stationary turbulence in the limit of vanishing kinematic viscosity ($\nu \rightarrow 0$), the Navier-Stokes equations predict an exact relationship between the third-order structure function and the energy dissipation rate $\bar{\epsilon}$ that scales linearly in the separation r namely,

$$\left\langle [\delta_L u]^3(\mathbf{x}, t; \mathbf{r}) \right\rangle = -\frac{4}{5} \bar{\epsilon} r . \quad (8)$$

Kolmogorov’s main hypotheses in deriving this relationship, which we now know as the four-fifths law were that (1) there exists an ‘inertial’ range of scales that are insensitive to the large flow-dependent scales and the viscous small scales, and (2) there exists a finite energy dissipation rate $\bar{\epsilon}$ in the limit of zero viscosity. The latter is known as the dissipation anomaly for Navier-Stokes turbulence. As noted in Uriel Frisch (1995, p. 76), Kolmogorov’s four-fifths law is “one of the most important results in fully developed turbulence because it is both exact and nontrivial. It thus constitutes a kind of ‘boundary condition’ on theories of turbulence: such theories, to be acceptable, must either satisfy the four-fifths law, or explicitly violate the assumptions made in deriving it.”

Kolmogorov then assumed the self-similarity of scales in the inertial range and was able to deduce, in steps that essentially amount to dimensional analysis, that the second-order structure function must scale with $r^{2/3}$ and that, consequently, the energy spectrum (which is essentially the Fourier transform of the second-order structure function) must scale as $k^{-5/3}$.

The equivalent of the Kármán-Howarth equation was derived for the LANS- α model in Holm (2002c).

Since the model relates the Helmholtz smoothed velocity \mathbf{u} to the unsmoothed velocity \mathbf{v} , the appropriate structure functions that emerge involve the second- and third-order two-point correlations between \mathbf{u} and \mathbf{v} . Upon following Kolmogorov’s analysis for isotropic inertial range statistics, the corollary to the LANS- α Kármán-Howarth equation is that solutions of the LANS- α equations possess two regimes of scaling, depending on whether the separation distance r is greater, or less, than the size α . First, we find that the corresponding four-fifths law for the LANS- α model has the following scaling behavior: For $r > \alpha$, the third-order structure function $\langle [\delta u(r)]^3 \rangle$ scales like r , thereby recovering Navier-Stokes behavior. In contrast, for $r < \alpha$, the third-order structure function scales like r^3 . If we then assume self-similarity, we find that, for $r > \alpha$, the second-order structure function scales like $r^{2/3}$, again recovering Navier-Stokes behavior. However, for $r < \alpha$, the second-order structure function scales like r^2 . Correspondingly, the power spectrum $E(k)$ for the smoothed velocity \mathbf{u} has two regimes, which transition from $k^{-5/3}$ for $k\alpha < 1$ to k^{-3} for $k\alpha > 1$. Thus, the Kármán-Howarth theorem for the LANS- α model is consistent with the spectral scaling results found for it in Foias et al. (2001) by dimensional arguments.

The $k^{-5/3} \rightarrow k^{-3}$ Spectral Scaling Transition and the LANS- α Dissipation Anomaly.

The LANS- α modification of Kolmogorov’s four-fifths law at small separations ($r < \alpha$) results from assuming the constancy of total LANS- α energy dissipation as $\nu \rightarrow 0$. This assumption corresponds to the energy dissipation anomaly for the LANS- α model. A technical argument using embedding theorems for Besov spaces² implies that the LANS- α total energy dissipation is indeed

constant as $\nu \rightarrow 0$ in three dimensions, provided its power spectrum $E(k)$ for kinetic energy is not steeper than k^{-4} . The k^{-3} spectrum for $k\alpha > 1$ is not too steep; therefore, the rolloff $k^{-5/3} \rightarrow k^{-3}$ in the LANS- α power spectrum is consistent with the necessary condition for possessing such an energy dissipation anomaly. Hence, the k^{-3} behavior in the power spectrum of the LANS- α model for $k\alpha > 1$ and the corresponding modification for separations $r < \alpha$ of Kolmogorov’s four-fifths law derived in (Holm 2002c) are both consistent with the assumption of constant dissipation of total kinetic energy as the Reynolds number tends to infinity.

The $k^{-5/3} \rightarrow k^{-3}$ Spectral Scaling Transition and Resolution

Requirements. The spectral scaling roll-off behavior for $k\alpha > 1$ has important implications for the computational performance of the LANS- α model. It substantiates the mathematical estimates of $Re^{3/2}$ for the number of degrees of freedom required for the LANS- α model to perform numerical simulations at a given Reynolds number in a periodic domain. According to this scaling, in two decades of numerical dynamic range, the LANS- α model should be able to simulate what would take three decades of numerical dynamic range for direct numerical simulation using the Navier-Stokes equations, provided the dissipation is chosen to properly balance the nonlinear transport at high wave numbers, $k\alpha \gg 1$.

Implications for Smoothness of LAE- α Solutions. The r^2 behavior of the longitudinal velocity structure functions for $r < \alpha$ in the limit of zero

² We are grateful to G. Eyink and E. S. Titi for discussions of this argument. See Constantin and Titi (1994) and Eyink (2004) for detailed discussions.

viscosity implies the LAE- α velocity is Lipschitz continuous (Hölder index $h = 1$). That is, the velocity gradients exist almost everywhere for the LAE- α model. In contrast, the velocity for the Navier-Stokes equations in the limit of zero viscosity (the Euler equations) has Hölder index $h = 1/3$, which gives no assurance of the existence of velocity gradients for the Euler equations. On the other hand, the viscous scaling regime for the Navier-Stokes equations has Hölder index $h = 1$ and the associated r^2 scaling agrees with that found in the inviscid LAE- α model. This agreement in scaling implies that, theoretically, velocity gradients in the LAE- α model are regularized to the same degree as viscosity regularizes the gradients in the Navier-Stokes equations. Corresponding results have been verified by analytical estimates in Marsden et al. (2000). The practical implications of these theoretical results would depend, of course, on the particular numerical implementation and on other relevant parameters of a computation.

The Lagrangian-Averaged Euler-Poincaré (LAEP) Theorem. The LAEP theorem was proved by Holm (2002a, 2002b). This theorem automates the derivation of the LANS- α model and explains its relation to the generalized Lagrangian mean (GLM) theory. The GLM equations provide the exact nonlinear dynamics of Lagrangian-averaged motion, but as mentioned earlier, they are not closed. Incorporating Taylor's classic hypothesis (1921) of frozen-in Lagrangian turbulent fluctuations into the GLM equations provides the closure and yields the LAE- α model. The LANS- α model description is then obtained by introducing dissipation in the form of Navier-Stokes viscosity.

This new derivation of the LANS- α model from GLM theory and the

LAEP theorem clarifies its relation to other models and shows how to extend the LANS- α model to include additional physical effects, such as rotation, buoyancy, compressibility, and magnetic fields. See Holm (2002a, 2002b) for more details.

Open Problems

Three issues have been raised in the results outlined here and in recent experience: How to understand and choose the length scale α , how to enhance our understanding of the interplay of nonlinear transport and eddy diffusion, and how to gain a more fundamental understanding of the implications of the Lagrangian-averaged fluctuation statistics of the trajectories by using data analysis.

The Length Scale α . Four heuristic interpretations for the length scale α have been proposed: (1) The size α is the length scale below which the smaller fluid circulations are swept by the larger ones and are not allowed to affect their own advection. This is the Taylor's hypothesis interpretation. (2) In the LES interpretation, the size α can be considered as a natural filter width, which defines the size of a "large" eddy in LES. (3) In its numerical interpretation, one practical rule of thumb has often been to choose α as some small integer multiple of the minimum grid spacing. In choosing α in this way, one maximizes the dynamic range left unmodified by the LANS- α model. (4) Because of its effect in slowing growth rates of instabilities at high wave numbers, Wingate (2003, Holm and Wingate 2003) suggested one could also choose the size α based on fluid and/or numerical stability requirements for numerical simulations.

All these interpretations lend heuristic insight into the physics of the particular problems we have studied using the LANS- α model.

However, the length scale α is a precisely defined statistical quantity obtained from first principles. The context of Lagrangian averaging, in which the length scale α is defined, provides the basis for future developments of the LANS- α model.

Statistical Context for Future Developments. The Lagrangian statistics of the trajectory fluctuations are related to the Eulerian velocity statistics at a fixed point in space. First, the equation for the fluctuation \mathbf{u}' in Eulerian velocity $\mathbf{u}(\mathbf{x}, t; \omega) = \bar{\mathbf{u}} + \mathbf{u}'(\mathbf{x}, t; \omega)$ for a random variable, ω , expressed in terms of the fluctuation $\xi(\mathbf{x}, t; \omega)$ in the Lagrangian trajectory away from its mean is given by Equation (9) in the accompanying box. This relation defines the deterministic time derivative operator, D/Dt , which does not depend on the random variable ω . As a result, one finds that the exact formula for the Lagrangian dispersion tensor $\langle \xi^k \xi^l \rangle$ in terms of the Eulerian velocity statistics at a fixed point in space is given by Equation (10), where $\langle \cdot \rangle = \int (\cdot) d\mu$ now denotes average over the probability measure $d\mu$ of the random process associated with ω . The trace of this formula, given by Equation (11) in the box, is Taylor's famous dispersion law (Taylor 1921) linking the Lagrangian and Eulerian statistics of turbulence at a fixed point in space. More discussion of the role played by Taylor's contributions in the development of the LANS- α model is given in the article "Taylor's Hypothesis, Hamilton's Principle and the LANS- α Model" on page 172. The anisotropic tensor version of this formula has yet to be applied in modeling turbulence using Lagrangian statistics, and it represents an open problem in turbulence modeling.

The constant alpha case derives from Equation (9) by substituting Taylor's hypothesis that the fluctuating circulations ξ are frozen into the

**Linking the Lagrangian and Eulerian
Statistics of Turbulence**

The Eulerian velocity fluctuation $\mathbf{u}'(\mathbf{x}, t; \omega)$ in terms of the Lagrangian-trajectory fluctuation $\xi(\mathbf{x}, t; \omega)$ is

$$\mathbf{u}'(\mathbf{x}, t; \omega) = \frac{\partial \xi}{\partial t} + \bar{\mathbf{u}} \cdot \nabla \xi - \xi \cdot \nabla \bar{\mathbf{u}} . \quad (9)$$

The total time derivative of the Lagrangian dispersion tensor is

$$\frac{d}{dt} \langle \xi^k \xi^l \rangle = \int \langle u'^k(0) u'^l(t) \rangle + \langle u'^l(0) u'^k(t) \rangle dt , \quad (10)$$

where $\langle \cdot \rangle = \int (\cdot) d\mu$ now denotes average over the probability measure $d\mu$ of the random process associated with ω .

The trace of Equation (10) yields Taylor's famous dispersions law linking Lagrangian and Eulerian statistics:

$$\frac{d}{dt} \langle |\xi|^2 \rangle = 2 \int \langle \mathbf{u}'(0) \cdot \mathbf{u}'(t) \rangle dt . \quad (11)$$

Eulerian mean flow, with velocity $\bar{\mathbf{u}}$,

$$\frac{d\bar{\xi}}{dt} + \bar{\mathbf{u}} \cdot \nabla \bar{\xi} = 0 . \quad (12)$$

Hence, one finds

$$\mathbf{u}'(\mathbf{x}, t; \omega) = -\xi \cdot \nabla \bar{\mathbf{u}} , \quad (13)$$

and, consequently,

$$\langle |\mathbf{u}'|^2 \rangle(\mathbf{x}, t) = \sum_{k,l} \langle \xi^k \xi^l \rangle \left(\frac{\partial \bar{\mathbf{u}}}{\partial \mathbf{x}^k} \cdot \frac{\partial \bar{\mathbf{u}}}{\partial \mathbf{x}^l} \right) . \quad (14)$$

The evolution of the symmetric tensor $\langle \xi^k \xi^l \rangle$ in this formula is specified by assuming a "flow rule" for the fluctuation statistics. This is the required closure step for the Lagrangian mean theories. For example, the Taylor hypothesis—see Equation (10)—of circulations being frozen into the Eulerian mean flow implies the flow rule for the symmetric tensor,

$$\frac{d}{dt} \langle \xi^k \xi^l \rangle = 0 , \quad (15)$$

which preserves the initial condition that these Lagrangian statistics are homogeneous and isotropic. That is, this flow rule preserves $\langle \xi^k \xi^l \rangle = \alpha^2 \delta^{kl}$, with a constant value of α . In this case, the mean kinetic energy of the turbulent circulations simplifies to the LANS- α form,

$$\langle |\mathbf{u}'|^2 \rangle = \alpha^2 |\nabla \bar{\mathbf{u}}|^2 , \quad (16)$$

which relates the kinetic energy of the Eulerian velocity fluctuations to the Lagrangian statistics and the mean shear.

Other flow rules for these Lagrangian statistics possessing more sophisticated evolution equations for $\langle \xi^k \xi^l \rangle$ were catalogued in Holm (1999). However, the results of these anisotropic-tensor α equations and their comparisons with the results for the LANS- α equations in the constant alpha case have yet to be systematically explored.

Nonlinear Transport vs Diffusion and Re Scaling. Most of the results presented in this review depend on a

trade-off between viscosity and non-linearity in modeling the average effects of the small scales on the large ones. Consider the energy dissipated by the LANS- α equations,

$$E_\alpha = \int \left[\frac{1}{2} |\mathbf{u}'|^2 + \frac{\alpha^2}{2} |\nabla \mathbf{u}'|^2 \right] d^3x . \quad (17)$$

Following the arguments of Foias et al. (2001), the two types of energy in Equation (17) become comparable at wave number $k\alpha \approx 1$, and the scaling of the kinetic energy spectrum rolls over from $E(k) \sim k^{-5/3}$ for $k\alpha < 1$ to $E(k) \sim k^{-3}$ for $k\alpha > 1$. This change of scaling produces two different inertial regimes for the LANS- α model, depending on whether the circulations are either larger or smaller than alpha. Consequently, the modified nonlinearity in the LANS- α model shortens the inertial range relative to the inertial range for the Navier-Stokes equations. For a fixed α , the second, steeper, k^{-3} inertial range for LANS- α ends when its nonlinear transport is balanced by viscous dissipation at a wave number κ_α . The LANS- α dissipation wave number κ_α scales with the Reynolds number as $\kappa_\alpha \sim Re^{1/2}$. This scaling is to be compared with the scaling for the Kolmogorov wave number $\kappa_{Ko} \sim Re^{3/4}$, at which dissipation balances nonlinearity for the Navier-Stokes equations. Thus, the modified nonlinearity of the LANS- α model strikes a balance with viscosity at a wave number that is lower than the wave number for the Navier-Stokes equations. In turn, the new balance of the LANS- α model produces energy spectra that agree well with the spectra produced by the Navier-Stokes balance at low wave numbers ($k\alpha < 1$), but the LANS- α spectra depart from the Navier-Stokes spectra at high wave numbers ($k\alpha \gg 1$), and thereby enhance the model's computability.

The scaling of dissipation wave number with Reynolds is $Re^{1/2}$ for this new balance vs $Re^{3/4}$ for the Navier-Stokes

balance. This difference in scaling is the source of the improved computability for the LANS- α model.

Flow Rules for Lagrangian

Statistics. The LANS- α model is, by definition, a mean field theory based on Lagrangian averaging, and Lagrangian averaging is still a young field. For example, the corresponding theory of large-deviation Lagrangian statistics for nonequilibrium processes has only recently begun to develop. New experiments and direct numerical simulations have recently begun to measure and investigate the fundamental tenets of Lagrangian trajectories in turbulence. One startling discovery in both experiments and simulations is that the Lagrangian trajectories tend to stay well localized along their mean trajectories for a long period, of the order of 30 Kolmogorov times (eddy turnover times at the dissipation scale). During this period, the Lagrangian trajectories tend to obey Taylor's hypothesis of frozen-in turbulence. Then, suddenly, large scale changes in the motion of those trajectories may occur, which apparently cause them to "forget" their previous history and start over. These experiments and simulations call for new studies of stochastic effects in Lagrangian turbulence that will take Lagrangian turbulence beyond its current status as a mean field theory. Perhaps the LANS- α model will be able to contribute as the mean field basis for these studies, and, thus, it may benefit from future achievements in this currently very active area. One potential benefit would be to include into a new generation of Lagrangian turbulence models the measured flow rules for the Lagrangian statistics that allow for the observed stochastic shifts, or punctuations, thereby occasionally and stochastically violating Taylor's deterministic hypothesis that the turbulence statistics remain frozen into the mean flow. One indication

that the LANS- α model may be able to form the basis for such an interpretation is the recent discovery (Jonathan Graham, Darryl Holm, Pablo Mininni, and Annick Pouquet, private communication, November 2004) that, when magnetic fields are included, this model possesses anomalous scaling, which is the hallmark of intermittency. ■

Acknowledgments

We are enormously grateful to our friends and collaborators in this endeavor. We are especially grateful to our advisory committee, S. Y. Chen, A. J. Domaradzky, R. Donnelly, G. Eyink, U. Frisch, R. M. Kerr, S. R. Sreenivasan and E. S. Titi, as well as to the participants in our four annual turbulence workshops. We thank them for their comments, encouragement and constructive suggestions. We are also grateful to our Turbulence Working Group members, who participated with us enthusiastically in weekly meetings. Finally, we are grateful to our respective divisions at Los Alamos and to STB Division, particularly David Watkins, for leadership and encouragement in providing key opportunities to make use of the unique facilities at Los Alamos.

Further Reading

Andrews, D. G., and M. E. McIntyre. 1978. An Exact Theory of Nonlinear Waves on a Lagrangian-Mean Flow. *J. Fluid Mech.* **89**: 609.

Barenblatt, G. I., and A. J. Chorin. 1998. Scaling Laws and Vanishing Viscosity Limits in Turbulence Theory. *SIAM Rev.* **40** (2): 265.

Barenblatt, G. I., A. J. Chorin, and V. M. Prostokishin. 1997. Scaling Laws in Fully Developed Turbulent Pipe Flow. *Appl. Mech. Rev.* **50**: 413.

Bleck, R. 2002. An Oceanic General Circulation Model Framed in Hybrid Isopycnic-Cartesian Coordinates. *Ocean Modell.* **37**: 55.

Bleck, R., and L. Smith. 1990. A Wind-Driven Isopycnic Coordinate Model of the North and Equatorial Atlantic Ocean. 1. Model Development and Supporting Experiments. *J. Geophys. Res.* **95** (C3): 3273.

Chen, Q., S. Y. Chen, and G. L. Eyink. 2003. The Joint Cascade of Energy and Helicity in Three-Dimensional Turbulence. *Phys. Fluids* **15**: 361.

Chen, Q., S. Y. Chen, G. L. Eyink, and D. D. Holm. 2003. Intermittency in the Joint Cascade of Energy and Helicity. *Phys. Rev. Lett.* **90** (21): 214503.

Chen, S. Y., C. Foias, D. D. Holm, L. G. Margolin, and R. Zhang. 1999. Direct Numerical Simulations of the Navier-Stokes Alpha Model. *Physica D* **133**: 66.

Chen, S. Y., C. Foias, D. D. Holm, E. J. Olson, E. S. Titi, and S. Wynne. 1998. The Camassa-Holm Equations as a Closure Model for Turbulent Channel and Pipe Flows. *Phys. Rev. Lett.* **81**: 5338.

———. 1999a. The Camassa-Holm Equations and Turbulence in Pipes and Channels. *Physica D* **133**: 49.

———. 1999b. A Connection Between the Camassa-Holm Equations and Turbulence in Pipes and Channels. *Phys. Fluids* **11**: 2343.

Cheskidov, A. 2002. Turbulent Boundary Layer Equations. *C. R. Acad. Ser. I* **334**: 423.

Cioranescu, D., and V. Girault. 1996. Variational and Classical Solutions of a Family of Fluids of Grade Two. *C. R. Acad. Ser. I* **322**: 1163.

———. 1997. Weak and Classical Solutions of a Family of Second Grade Fluids. *Int. J. Non-Linear Mech.* **32**: 317.

Clark, R. A., J. H. Ferziger, and W. C. Reynolds. 1979. Evaluation of Subgrid-Scale Models Using an Accurately Simulated Turbulent Flow. *J. Fluid Mech.* **91**: 1.

Constantin, P., Weinan E, and E. S. Titi. 1994. Onsager's Conjecture on the Energy Conservation for Solutions of Euler's Equation. *Commun. Math. Phys.* **165**: 207.

- Danabasoglu, G., and J. C. McWilliams. 2000. An Upper-Ocean Model for Short-Term Climate Variability. *J. Climate* **13**: 3380.
- Domaradzki, J. A., and D. D. Holm. 2001. Navier-Stokes-Alpha Model: LES Equations with Nonlinear Dispersion. In *Modern Simulation Strategies for Turbulent Flow*. p. 107. Edited by B. J. Geurts. Flourtown, PA: R. T. Edwards, Inc.
- Domaradzki, J. A., and E. M. Saiki. 1997. A Subgrid-Scale Model Based on the Estimation of Unresolved Scales of Turbulence. *Phys. Fluids* **13**: 2148.
- Dukowicz, J. K., and R. D. Smith. 1994. Implicit Free-Surface Method for the Bryan-Cox-Semtner Ocean Model. *J. Geophys. Res. – Oceans* **99** (C4): 7991.
- . 1996. Stochastic Theory of Compressible Turbulent Fluid Transport. *Phys. Fluids* **99**: 7991.
- Dunn, J. E., and R. L. Fosdick. 1974. Thermodynamics, Stability, and Boundedness of Fluids of Complexity 2 and Fluids of Second Grade. *Arch. Rat. Mech. Anal.* **56**: 191.
- Eyink, G. L. 2003. Local 4/5-Law and Energy Dissipation Anomaly in Turbulence. *Nonlinearity* **16**: 137.
- Eyink, G. L., and K. R. Sreenivasan. 2004. Onsager and the Theory of Hydrodynamic Turbulence. To appear in *Rev. Mod. Phys.*
- Fabijonas, B., and D. D. Holm. 2003. Mean Effects of Turbulence on Elliptical Instability. *Phys. Rev. Lett.* **90**: 124501.
- . 2004a. Craik-Criminale Solutions and Elliptic Instability in Nonlinear-Reactive Closure Models for Turbulence. *Phys. Fluids* **16**: 853.
- . 2004b. Multi-Frequency Craik-Criminale Solutions of the Navier-Stokes Equations. *J. Fluid Mech.* **506**: 207.
- . 2004c. Euler-Poincaré Formulation and Elliptic Instability for n th-Gradient Fluids. *J. Phys. A* **37**: 7609.
- Foias, C., D. D. Holm, and E. S. Titi. 2001. The Navier-Stokes-Alpha Model of Fluid Turbulence. *Physica D* **152**: 505.
- . 2002. The Three Dimensional Viscous Camassa-Holm Equations, and Their Relation to the Navier-Stokes Equations and Turbulence Theory. *J. Diff. Eqs.* **14**: 1.
- Frisch, U. 1995. *Turbulence—The Legacy of A. N. Kolmogorov*. Cambridge, UK: Cambridge University Press.
- Gallavotti, G. 1993. Some Rigorous Results About 3D Navier-Stokes. In *Les Houches 1992 NATO-ASI. Meeting on Turbulence in Extended Systems*. p. 45. Edited by R. Benzi, C. Basdevant, and S. Ciliberto. New York: Nova Science Publishers.
- Gatski, T. B., and C. G. Speziale. 1993. On Explicit Algebraic Stress Models for Complex Turbulent Flows. *J. Fluid Mech.* **254**: 59.
- Gent, P. R., and J. C. McWilliams. 1990. Isopycnal Mixing in Ocean Circulation Models. *J. Phys. Oceanogr.* **20**: 150.
- Gent, P. R., F. O. Bryan, G. Danabasoglu, S. C. Doney, W. R. Holland, W. G. Large, and J. C. McWilliams. 1998. The NCAR Climate System Model Global Ocean Component. *J. Climate* **11**: 1287.
- Geurts, B. J., and D. D. Holm. 2002a. Alpha-Modeling Strategy for LES of Turbulent Mixing. In *Turbulent Flow Computation*. p. 237. Edited by D. Drikakis and B. J. Geurts. London: Kluwer Academic Publishers.
- . 2002b. Leray Simulation of Turbulent Shear Layers. In *Advances in Turbulence IX: Proceedings of the Ninth European Turbulence Conference*. p. 337. Edited by J. P. Castro and P. E. Hancock. Barcelona: CIMNE.
- . 2003a. Regularization Modeling for Large-Eddy Simulation. *Phys. Fluids* **15**: L13.
- . 2003b. Commutator-Errors in Large-Eddy Simulation. Submitted to *Phys. Fluids*.
- Gill, A. E. 1982. *Atmosphere-Ocean Dynamics*. San Diego, CA: Academic Press.
- Gjaja, I., and D. D. Holm. 1996. Self-Consistent Wave-Mean Flow Interaction Dynamics and its Hamiltonian Formulation for a Rotating Stratified Incompressible Fluid. *Physica D* **98**: 343.
- Greatbatch, R. J., and B. T. Nadiga. 2000. Four Gyre Circulation in a Barotropic Model with Double Gyre Wind Forcing. *J. Phys. Oceanogr.* **30**: 1461.
- Gutmark, E., and I. Wygnanski. 1976. Planar Turbulent Jet. *J. Fluid Mech.* **73**: 465.
- Holm, D. D. 1996. Hamiltonian Balance Equations. *Physica D* **98**: 379.
- . 1999. Fluctuation Effects on 3D Lagrangian Mean and Eulerian Mean Fluid Motion. *Physica D* **133**: 215.
- . 2002a. Variational Principles for Lagrangian Averaged Fluid Dynamics. *J. Phys. A* **35**: 1.
- . 2002b. Averaged Lagrangians and the Mean Dynamical Effects of Fluctuations in Continuum Mechanics. *Physica D* **170**: 253.
- . 2002c. Kármán-Howarth Theorem for the Lagrangian-Averaged Navier-Stokes-Alpha Model of Turbulence. *J. Fluid Mech.* **467**: 205.
- . 2003. Modified Speziale Model for LES Turbulence. Submitted to *J. Fluid Mech.*
- Holm, D. D., and R. M. Kerr. 2002. Transient Vortex Events in the Initial Value Problem for Turbulence. *Phys. Rev. Lett.* **88** (24): 244501.
- Holm, D. D., and B. Nadiga. 2003. Modeling Mesoscale Turbulence in the Barotropic Double Gyre Circulation. *J. Phys. Oceanogr.* **33**: 2355.
- Holm, D. D., and B. A. Wingate. 2004. Baroclinic Instability for LANS-Alpha Models. To appear in *J. Phys. Oceanogr.*
- Holm, D. D., J. E. Marsden, and T. S. Ratiu. 1998a. Euler-Poincaré Models of Ideal Fluids with Nonlinear Dispersion. *Phys. Rev. Lett.* **80**: 4173.
- . 1998b. Euler-Poincaré Equations and Semidirect Products with Applications to Continuum Theories. *Adv. Math.* **137**: 1.
- . 2002. The Euler-Poincaré Equations in Geophysical Fluid Dynamics. In *Large-Scale Atmosphere-Ocean Dynamics 2: Geometric Methods and Models*. p. 251. Edited by J. Norbury and I. Roulstone. Cambridge, UK: Cambridge University Press.

- Holm, D. D., V. Putkaradze, P. D. Weidman, and B. A. Wingate. 2003. Boundary Effects on Exact Solutions of the Lagrangian-Averaged Navier-Stokes- α Equations. *J. Stat. Phys.* **113**: 841.
- Horiuti, K. 2002. Roles of Nonaligned Eigenvectors of Strain-Rate and Subgrid-Scale Stress Tensors for Turbulence Generation. Submitted to *J. Fluid Mech.*
- Kolmogorov, A. N. 1941a. The Local Structure of Turbulence in Incompressible Viscous Fluid for Very Large Reynolds Numbers. *Dok. Akad. Nauk. SSSR* **30**: 4. English translation *Proc. R. Soc. London, Ser. A* 1991, **434**: 9.
- . 1941b. Dissipation of Energy in the Locally Isotropic Turbulence. *Dok. Akad. Nauk. SSSR* **32**: 1. English translation *Proc. R. Soc. London, Ser. A*, 1991, **434**: 15.
- Krahmann, G., and M. Visbeck. 2003. Labrador Sea Deep Convection Experiment Data Collection. Sponsored by the Office of Naval Research. [Online]: <http://www.ldeo.columbia.edu/~visbeck/labsea/labsea.html>
- Kurien, S. 2003. The Reflection-Antisymmetric Counterpart of the Kármán-Howarth Theorem. *Physica D* **175**: 167.
- Lauder, B. E., and D. B. Spalding. 1974. The Numerical Computation of Turbulent Flows. *Comput. Methods Appl. Mech. Engr.* **3**: 269.
- Leonard, A. 1974 Energy Cascade in Large-Eddy Simulations of Turbulent Fluid Flows. *Adv. Geophys.* **18**: 237.
- Leray, J. 1934. Sur le Mouvement d'un Liquide Visqueux Emplissant L'espace. *Acta Math.* **63**: 193. Reviewed in P. Constantin, C. Foias, B. Nicolaenko and R. Temam. 1989. *Integral Manifolds and Inertial Manifolds for Dissipative Partial Differential Equations, Applied Mathematical Sciences*. Vol. 70. New York: Springer-Verlag
- Lorenz, E. N. 1992. The Slow Manifold—What Is It? *J. Atmos. Sci.* **49**: 2449.
- Lumley, J. L. 1970. Toward a Turbulent Constitutive Relation. *J. Fluid Mech.* **41**: 413.
- Marsden, J. E., T. S. Ratiu, and S. Shkoller. 2000. The Geometry and Analysis of the Averaged Euler Equations and a New Diffeomorphism Group. *Geom. Funct. Anal.* **10**: 582.
- Marsden, J. E., and S. Shkoller. 2001. Global Well-Posedness for the Lagrangian Averaged Navier-Stokes (LANS-alpha) Equations on Bounded Domains. *Philos. Trans. R. Soc. London, Ser. A* **359**: 1449.
- Meneveau, C., and J. Katz. 2000. Scale-Invariance and Turbulence Models for Large-Eddy Simulation. *Annu. Rev. Fluid Mech.* **32**: 1.
- Mohseni, K., B. Kosovic, J. E. Marsden, and S. Shkoller. 2001. Numerical Simulations of Forced Homogeneous Turbulence Using Lagrangian Averaged Navier-Stokes Equations. In *Proceedings of the 15th AIAA Computational Fluid Dynamics Conference*, AIAA Paper 2001-2645. Anaheim, CA: AIAA.
- Mohseni, K., B. Kosovic, J. E. Marsden, S. Shkoller, D. Carati, A. Wray, and R. Rogallo. 2000. Numerical Simulations of Homogeneous Turbulence Using Lagrangian Averaged Navier-Stokes Equations. In *Center for Turbulence Research Proceedings of the 2000 Summer Program*. p. 271. NASA Ames Research Center/Stanford University.
- Nadiga, B. T. 2000. Scaling Properties of an Inviscid Mean-Motion Fluid Model. *J. Stat. Phys.* **98**: 935.
- Nadiga, B. T., and L. G. Margolin. 2001. Dispersive Eddy Parameterization in a Barotropic Ocean Model. *J. Phys. Oceanogr.* **31**: 2525.
- Nadiga, B. T. and S. Shkoller 2001. Enhancement of the Inverse-Cascade of Energy in the Two-Dimensional Averaged Euler Equations. *Phys. Fluids* **13**: 1528.
- Onsager, L. 1949. Statistical Hydrodynamics. *Nuovo Cimento* (Supplement) **6**: 279.
- Pacanowski, R. C. 1995. MOM 2 Documentation, User's Guide and Reference Manual, Version 1.0x. Geophysical Fluid Dynamics Laboratory Ocean Group Technical Report 3. Geophysical Fluid Dynamics Laboratory/NOAA, Princeton University, Princeton, NJ.
- Putkaradze, V., and P. Weidman. 2003. Turbulent Wake Solutions of the Prandtl-Alpha Equations. *Phys. Rev. E* **67**: 036304.
- Rivlin, R. S. 1957. The Relation Between the Flow of Non-Newtonian Fluids and Turbulent Newtonian Fluids. *J. Rat. Mech. Anal.* **15**: 213.
- Smagorinsky, J. 1963. General Circulation Experiments with the Primitive Equations. *Mon. Weather Rev.* **93**: 99.
- Speziale, C. G. 1991. Analytical Methods for the Development of Reynolds-Stress Closures in Turbulence. *Annu. Rev. Fluid Mech.* **23**: 107.
- . 1998. Turbulence Modeling for Time-Dependent RANS and VLES: A Review. *AIAA J.* **36**: 173.
- Taylor, G. I. 1921. Diffusion by Continuous Movements. *Proc. London Math. Soc.* **20**: 196.
- Taylor, M., S. Kurien, and G. Eyink. 2003. Recovering Isotropic Statistics in Turbulence Simulations: The Kolmogorov 4/5th-Law. *Phys. Rev. E* **68**: 026310.

- Vreman, B., B. Geurts, and H. Kuerten. 1996. Large Eddy Simulation of the Temporal Mixing Layer Using the Clark Model. *Theor. Comput. Fluid Dyn.* **8**: 309.
- Winckelmans, G. S., A. A. Wray, O. V. Vasilyev, and H. Jeanmart. 2001. Explicit-Filtering Large-Eddy Simulation Using the Tensor-Diffusivity Model Supplemented by a Dynamic Smagorinsky Term. *Phys. Fluids* **13**: 1385.
- Wingate, B. A. 2003. Numerical Analysis of the LA Shallow Water Models. Submitted to *J. Comp. Phys.*
- Zagarola, M. V. 1996. "Mean Flow Scaling of Turbulent Pipe Flow." Ph.D. thesis. Department of Mechanical and Aerospace Engineering, Princeton University.

*For further information, contact
Darryl D. Holm (505) 667-6398
(dholm@lanl.gov) or Beth A. Wingate
(505) 665-7869 (wingate@lanl.gov).*